Andean Geology 52 (1): 117-134. January, 2025
doi: 10.5027/andgeoV52n1-3675

Andean Geology
www.andeangeology.cl

The Isomass Method: Verifying conserved elements in geochemically open geological processes

***Sergio Calderón-Díaz[1, 2, 3, 4], Brian Townley[2], Cliford R. Stanley[5]**

[1] *Escuela de Geología, Facultad de Ingeniería, Universidad Santo Tomás, Ejército 146, Santiago, Chile.*
Orcid ID:https://orcid.org/0000-0002-4410-478X
sergio.ernesto.calderon.diaz@gmail.com
[2] *Departamento de Geología, Facultad de Ciencias Físicas y Matemáticas, Universidad de Chile, Plaza Ercilla 803, Santiago, Chile.*
btownley@cec.uchile.cl
[3] *Instituto de Geografía, Facultad de Ciencias del Mar y Geografía, Pontificia Universidad Católica de Valparaíso, Av. Brasil 2241, Valparaíso, Chile.*
[4] *Carrera de Derecho, Facultad de Ciencias Sociales, Universidad de Playa Ancha, Gran Bretaña 20, Valparaíso, Chile.*
[5] *Department of Earth and Environmental Science, Acadia University, 12 University Ave., Wolfville, Nova Scotia, Canada.*
cliff.stanley@acadiau.ca

* *Corresponding author: sergio.ernesto.calderon.diaz@gmail.com*

ABSTRACT. This contribution presents the Isomass method, aimed at verifying the conserved behaviour of elements in geochemically open systems even when the parent rock composition is lacking. The method estimates system size changes for a specific element that is assumed to be conserved by calculating the amount of material transfer for each of the other elements, thus verifying (or rejecting) the initial assumption. By analysing the calculated amount of material transfer (or daughter system size ratios), additional conserved elements (if any) can be identified. The Isomass method is used here to evaluate a set of numerically generated samples whose element concentrations derived after mass additions and losses are assigned to daughter rocks. In addition, it is also applied to three real datasets that examine soil formation, magmatic fractionation in a komatiitic lava, and hydrothermal metasomatism. The method is capable of: (1) determining which elements confirm their conserved behaviour for a variety of geological environments; (2) identifying which other elements are conserved, added or lost; (3) calculating the amount of material transfer; and (4) providing a measure of the extent of the conserved character of elements. The method illustrates that the whole-rock compositions of parent and daughter samples do not represent the actual material transfer that occurred during geochemically open geological processes, as conserved elements may appear enriched or depleted, and non-conserved elements may have concentrations that do not reflect the actual material transfers that took place. The Isomass method is therefore a proper and valuable tool for the verification of conserved elements and the investigation of material transfer in rocks.

Keywords: Isomass, Conserved element, Material transfer, Concentration, Closure.

RESUMEN. El método Isomasas: verificando elementos conservados en procesos geológicos geoquímicamente abiertos. Esta contribución presenta el método de Isomasas, enfocado en verificar el comportamiento conservado de elementos en sistemas geoquímicamente abiertos, incluso cuando no se encuentra disponible la composición de la roca parental. El método estima los cambios en el tamaño del sistema para un elemento específico que se asume conservado, calculando la cantidad de transferencia de material para cada uno de los otros elementos, verificando (o rechazando) así la suposición inicial. Al analizar la cantidad calculada de transferencia de material (o las proporciones de tamaño del sistema hijo), se pueden identificar los elementos conservados adicionales, en caso de que los haya. El método de Isomasas se utiliza aquí para evaluar un conjunto de muestras generadas numéricamente, cuyas concentraciones elementales derivadas después de la adición y pérdida de masa son asignadas a las rocas hijas. Además, también se aplica a tres conjuntos de datos reales que examinan formación del suelo, fraccionamiento magmático en una lava komatítica y metasomatismo hidrotermal. El método es capaz de lo siguiente: (1) determinar qué elementos confirman su comportamiento conservado para una variedad de ambientes geológicos; (2) identificar qué otros elementos son conservados, añadidos o perdidos; (3) calcular la cantidad de transferencia de material; y (4) proporcionar una medida del alcance del carácter conservado de los elementos. El método ilustra que las composiciones de roca total de las muestras parental e hija no son representativas de la transferencia real de material que ocurrió durante procesos geológicos geoquímicamente abiertos, dado que los elementos conservados pueden aparecer enriquecidos o empobrecidos, y los elementos no conservados pueden exhibir concentraciones que no reflejen las transferencias de material que tuvieron lugar. El método de Isomasas es, por tanto, una herramienta de utilidad para la verificación de elementos conservados y para la investigación de la transferencia de material en rocas.

Palabras clave: Isomasa, Elemento conservado, Transferencia de material, Concentración, Clausura.

1. Introduction

Over the last seventy years, material transfer processes have been a major issue in a variety of geological problems. In alteration systems, for example, calculation of the extent of element mobility has been the subject of many studies (*e.g.*, Gresens, 1967; Giggenbach, 1984; Grant, 1986). The main limitation in these studies has been theoretical, since the mobility of elements is estimated directly from element concentrations. This problem is compounded due to closure conditions (*e.g.*, Pearce, 1968; Russell and Nichols, 1988; Russell and Stanley, 1990), and because any concentration variations are dependent not only upon the amount of material transfer of each element but also the size change of the system.

Chemical material transfer processes are responsible for the formation of most mineral deposits, and are also important in magmatic, metamorphic, sedimentary, and metasomatic phenomena. The effects of these processes on the lithogeochemistry of rocks have been analysed among others by Brinkley (1946, 1947), Giggenbach (1984), Ghiorso (1985), and Karpov *et al*. (1997, and references therein). The main objective of these studies was the characterization of the nature of material transfer so as to provide constraints on the source of elements added to or lost from these rocks, and to better understand the fluid-mineral equilibria that drove the material transfer.

Lithogeochemical studies in mineral exploration have stressed the identification and practical use of immobile elements (MacLean and Barrett, 1993; and references therein) during hydrothermal alteration and metasomatism (Maclean, 1990). MacLean and Kranidiotis (1987) claimed that a pair of incompatible elements should lie on a well correlated (*i.e.*, R>0.9) linear trend, ideally passing through the origin in a chemical system derived from a single protolith (or precursor; MacLean and Barrett, 1993), or passing through the error ellipses of the data (Stanley and Russell, 1989), to be regarded as immobile during fractionation. Any linear trend away from the precursor composition is the result of a net material transfer (addition or loss) in the whole system size, resulting in the dilution or enrichment of elements as intensive variables (see figures 1 and 4 in MacLean and Barrett, 1993).

To tackle this problem, around forty years ago Grant (1986) presented the Isocon method following Gresens (1967). This method compared the chemical composition of a fresh versus an altered sample in a plot that recognized an immobile element if the concentration in the fresh and in the altered systems were the same. The line joining the origin with the immobile element coordinates was called the isocon (hence the name of the method). The departure from that line was interpreted as enrichment or dilution. More recently, Guo *et al*. (2009) and Hilchie *et al*. (2018) proved that the Isocon method could be transformed, standardized, and compared with Pearce Element Ratio (PER) analyses to reveal stoichiometrically meaningful material transfer behaviours. PER analysis is a technique that exploits the principles of projective geometry to identify the appropriate location(s) in geochemical space from which to examine lithogeochemical data, through the assumption of a conserved element (Russel *et al*., 1990).

This contribution describes how to verify conserved element behaviour amongst elements with potential immobility (Vistelius and Sarmanov, 1961; Pearce, 1968; Russell and Nichols, 1988). The Isomass method is therefore presented. To illustrate its usefulness and potential uses, the method is applied here to a set of numerically generated samples that allow quantification of material transfer in a geochemically open system. It is also applied to a variety of published datasets to track how well the method performs in real-case scenarios. The model evaluates the whole-rock concentrations of potentially conserved elements in parent and daughter samples. Starting from the mass balance equation of Grant (1986), it derives an equation that quantitatively estimates the mass balance for every (conserved or added/lost) element in the system. The main questions associated with this method are determining: (1) which samples are related to each other via material transfer (*i.e.*, are cogenetic) (Russell and Nichols, 1988); (2) which of the parent samples represents the 'best' original rock composition; and (3) how analytical error affects the above procedures. The method, its theoretical foundations, applications, and limitations are presented below.

2. Theory: Mass transfer and the isomass approach

In 1967, Randall Gresens presented the first equation that calculated the amount of element loss or gain between two parent-daughter samples by using element concentrations from an n-dimensional compositional system under the assumption of constant volume (Gresens, 1967). Some twenty years later, Grant (1986) solved Gresens' equation by following an alternative conserved-element strategy, presenting the Isocon method as a result. This new approach was then improved both mathematically and graphically by determining the "best" scaling factors (conserved elements) to construct the Isocon line (*e.g.*, Baumgartner and Olsen, 1995; Mukherjee and Gupta, 2007) (see Introduction). As these improved methodologies documented the relationship between mass and composition, we introduce here a technique to estimate the actual material transfer during geochemically open geological processes. The development of the new set of equations is explained as follows.

The Grant (1986) formulation is given by:

$$(1) \qquad X_{pi} + dX_i = X_{di}$$

where X_{pi} represents the mass of element *i* in the parent (or unaltered) rock sample, X_{di} is the mass of element *i* in the daughter (or altered) rock sample, and dX_i refers to the amount of material of the i^{th} element that was added ($dX_i>0$) or lost ($dX_i>0$). After dividing both sides of Equation (1) by the system size (mass) of the daughter rock (S_d) and multiplying the left side by S_p/S_p, with S_p being the system size (mass) of the parent rock, we obtain:

$$(2) \qquad \left(\frac{S_p}{S_d}\cdot\frac{X_{pi}}{S_p}\right) + \left(\frac{S_p}{S_d}\cdot\frac{dX_i}{S_p}\right) = \frac{X_{di}}{S_d}$$

The system sizes S_p and S_d are the sums of the masses of the elements present in the parent and daughter rocks, respectively. These terms can be expressed as $S_j=\sum_{i=1}^{n} X_{ji}$, where *j* can be *p* or *d* accordingly. Because the concentration of element *i* in any rock means $x_{ji}=X_{ji}/S_j$, Equation (2) becomes:

$$(3) \qquad x_{di} = \frac{S_p}{S_d}\left(x_{pi} + \frac{dX_i}{S_p}\right)$$

Grant (1986, 2005), Baumgartner and Olsen (1995), Coelho (2006), and Mukherjee and Gupta (2007), among others, considered the identity:

$$(4) \qquad \frac{dX_i}{S_p} = dx_i$$

which is true only when the parent and daughter system sizes are equal (*i.e.*, the material transfer process is a perfect mass exchange). This condition is unlikely in open systems because any change in the concentration of an element is a function of the mass change of that element and the mass change of the system as a whole (*e.g.*, Russell and Stanley, 1990). The Isocon equation of Grant (1986) is obtained by imposing $dX_k=0$ in Equation (3) for a hypothetical conserved element *k*. This means:

$$(5) \qquad x_{dk} = \frac{S_p}{S_d} x_{pk}$$

When these data are plotted on a diagram, the mobility of the different chemical species can be determined by means of their vertical distances to the line defined by the Isocon slope (S_p/S_d), which is the line joining the origin with the immobile element coordinates (x_{pk}, x_{dk}) (Grant 2005). This formulation implies that all elements falling on the Isocon line are conserved, however, it might still be possible for certain elements to fall on the Isocon even if they experienced a mass change during an alteration event. This can be due to the combined effect of the mass change itself and that of the whole system.

To avoid the hindrances from above, we redistributed the terms of Equation (3) so the daughter system size (S_{dk}) for a hypothetically conserved element can be estimated:

$$S_{dk} = \frac{x_{pk}}{x_{dk}} S_p \tag{6}$$

By knowing S_{dk} it is possible to estimate the mass of each element in the daughter system from an arbitrary parent mass as:

$$X_{di} = S_{dk} x_{di} \tag{7}$$

The concept of Isomass is related to the fact that the mass of the element hypothetically considered as conserved is equal both in the parent and daughter systems (*i.e.*, $X_{dk}=X_{pk}$). The mass difference of any i th element when comparing the daughter and the parent rocks (X_{di}-X_{pi}=dX_i) represents a quantitative estimation of the element material transfer. By definition, the conserved element k will have null material transfer, however, if the resulting dX_k obtained after equations (7) and (1) is not equal to zero, then the hypothesis is no longer valid, the selected element is not conserved, and another element must therefore be tested.

Those elements that overestimate the mass of the daughter system ($S_{di}/S_{dk} > 1$) and have negative element mass differences ($dX_i < 0$) are referred to as *lost* elements. Likewise, those that underestimate the mass of the daughter system ($S_{di}/S_{dk} < 1$) and have positive element mass differences ($dX_i > 0$) are referred to as *added* elements. The value (S_{di}/S_{dk}) is called the *daughter system size ratio*. Note that this value is different for each element and for each daughter sample, as $S_{di}/S_{dk} = {}^{x_{pi}/x_{di}}\!\big/_{x_{pk}/x_{dk}}$ for a specific sample pair.

In order to determine which elements are the most added (or lost), the relative material transfer needs to be calculated. This parameter is usually expressed as $dr_i = dX_i/X_{pi}$ and represented in percentage form (cf. Stanley, 1993). It can then be compared across elements to ascertain which are contributing the most to the observed changes in system size.

As a rule, only the conserved element will correctly estimate the daughter system size (see Equation 6). The ultimate criterion to identify the conserved group of elements involves finding those elements capable of fulfilling the following requirements: (1) the calculated element material transfer (dX_k) or the relative material transfer (dr_k) are smaller than measurement error; (2) the estimated daughter system size ratios (S_{di}/S_{dk}) are also smaller than measurement error; and (3) the daughter system size ratios calculated for two hypothetically conserved elements k_1 and k_2 should be nearly identical for every sample and element (*i.e.*, they exhibit the highest correlation, a best-fit slope closest to unity, and a best-fit intercept closest to zero).

3. Results

3.1. Numerically generated case

The numerically generated dataset is presented in table 1. The computer code and source files needed to perform these calculations are available in Supplementary material 1. This dataset has been evaluated using the Isomass method described above to illustrate how it works (Table 2), besides its benefits, implications, and limitations.

The numerically generated parent rock contained 16 elements (11 major oxides and 5 trace elements). It was generated by assuming an initial rock mass (S_p) of 100 g (Table 1). This parent rock was subject to material transfer, producing seven daughter rocks (Alter 1 to Alter 7 in Table 1) with new element masses (S_{di}). Only the masses of TiO_2 and Zr remained constant and are thus said to be conserved. The system size of some of these daughter samples (Alter 1 to Alter 3) decreased when compared to the parent rock, whereas the size of the others increased (Alter 4 to Alter 7). These parent and daughter element masses were then converted into concentrations and normalized to 100%, producing concentrations in weight percentage (wt%) for the major oxides and parts per million units (ppm) for the trace elements (Table 1). This numerically generated dataset is meant to represent typical whole-rock analysis results obtained in routine lithogeochemical surveys.

TABLE 1. NUMERICALLY GENERATED CASE.

	Mass X_i (g)											Mass X_i (g)					Total (g)	Dauther system size difference
i	**SiO_2**	**TiO_2**	**Al_2O_3**	**FeO**	**Fe_2O_3**	**MnO**	**MgO**	**CaO**	**Na_2O**	**K_2O**	**P_2O_5**	**Sc**	**Li**	**Rb**	**Sr**	**Zr**	S_j	S_d-S_p
Precursor	54.38	1.027	17.72	4.56	4.28	0.23	4.84	6.96	3.83	1.91	0.20	0.000	0.007	0.049	0.010	0.008	100.00	0.00
Alter 1	50.00	1.027	16.00	4.00	4.00	0.10	4.00	6.00	3.00	1.00	0.10	0.000	0.006	0.040	0.008	0.008	89.29	-10.71
Alter 2	45.00	1.027	14.00	3.00	3.00	0.08	3.00	3.00	2.00	0.80	0.08	0.000	0.005	0.035	0.007	0.008	75.04	-24.96
Alter 3	40.00	1.027	12.00	2.50	2.50	0.06	2.50	2.50	1.50	0.60	0.06	0.000	0.004	0.030	0.006	0.008	65.30	-34.70
Alter 4	60.00	1.027	19.00	5.00	5.00	0.30	5.50	8.00	4.50	2.50	0.30	0.001	0.008	0.060	0.011	0.008	111.22	11.22
Alter 5	65.00	1.027	20.00	6.00	6.00	0.40	6.00	9.00	5.00	3.00	0.40	0.001	0.009	0.070	0.012	0.008	121.93	21.93
Alter 6	70.00	1.027	21.00	7.00	7.00	0.50	7.00	10.00	6.00	4.00	0.50	0.001	0.010	0.075	0.013	0.008	134.13	34.13
Alter 7	75.00	1.027	22.00	8.00	8.00	0.60	8.00	11.00	7.00	5.00	0.60	0.001	0.011	0.080	0.014	0.008	146.34	46.34

	Concentration x_i (wt%)											Concentration x_i (ppm)					Total (%)
i	**SiO_2**	**TiO_2**	**Al_2O_3**	**FeO**	**Fe_2O_3**	**MnO**	**MgO**	**CaO**	**Na_2O**	**K_2O**	**P_2O_5**	**Sc**	**Li**	**Rb**	**Sr**	**Zr**	
Precursor	54.38	1.03	17.72	4.56	4.28	0.23	4.84	6.96	3.83	1.91	0.20	3.980	74.000	488.000	96.000	83.027	100.00
Alter 1	56.00	1.15	17.92	4.48	4.48	0.11	4.48	6.72	3.36	1.12	0.11	3.920	67.197	447.978	89.596	92.986	100.00
Alter 2	59.97	1.37	18.66	4.00	4.00	0.11	4.00	4.00	2.67	1.07	0.11	5.064	66.628	466.398	93.280	110.639	100.00
Alter 3	61.26	1.57	18.38	3.83	3.83	0.09	3.83	3.83	2.30	0.92	0.09	5.360	61.259	459.445	91.889	127.155	100.00
Alter 4	53.95	0.92	17.08	4.50	4.50	0.27	4.95	7.19	4.05	2.25	0.27	4.496	71.933	539.494	98.907	74.654	100.00
Alter 5	53.31	0.84	16.40	4.92	4.92	0.33	4.92	7.38	4.10	2.46	0.33	4.921	73.814	574.112	98.419	68.095	100.00
Alter 6	52.19	0.77	15.66	5.22	5.22	0.37	5.22	7.46	4.47	2.98	0.37	5.219	74.552	559.140	96.918	61.898	100.00
Alter 7	51.25	0.70	15.03	5.47	5.47	0.41	5.47	7.52	4.78	3.42	0.41	5.467	75.167	546.666	95.667	56.735	100.00

Mass (g), weight percent (wt%) and parts per million (ppm) data for an initial precursor (parent) composition affected by general loss (Alter 1-3) and general addition (Alter 4-7) of mass. Daughter-parent system size differences are indicated as well.

TABLE 2. DAUGHTER SYSTEM SIZES (IN GRAMS) AND RELATIVE MATERIAL TRANSFER FOR ALL ELEMENTS WHEN TIO_2, ZR, AL_2O_3, SR, AND P_2O_5 ARE INDIVIDUALLY ASSUMED AS CONSERVED.

S_{dk} (g)

k	SiO_2	TiO_2	Al_2O_3	FeO	Fe_2O_3	MnO	MgO	CaO	Na_2O	K_2O	P_2O_5	Sc	Li	Rb	Sr	Zr
Alter 1	97.12	89.29	98.87	101.70	95.45	203.87	107.96	103.63	113.98	170.73	176.07	101.54	110.12	108.93	107.15	89.29
Alter 2	90.69	75.04	94.96	113.97	106.96	214.18	120.98	174.20	143.69	179.36	184.97	78.60	111.06	104.63	102.92	75.04
Alter 3	88.77	65.30	96.40	119.00	111.68	248.48	126.32	181.89	166.71	208.09	214.59	74.25	120.80	106.22	104.47	65.30
Alter 4	100.80	111.22	103.70	101.34	95.11	84.64	97.80	96.81	94.65	85.06	73.10	88.53	102.87	90.46	97.06	111.22
Alter 5	102.01	121.93	108.00	92.59	86.89	69.60	98.28	94.34	93.39	77.71	60.11	80.88	100.25	85.00	97.54	121.93
Alter 6	104.21	134.13	113.16	87.30	81.93	61.25	92.67	93.41	85.61	64.12	52.90	76.27	99.26	87.28	99.05	134.13
Alter 7	106.11	146.34	117.84	83.34	78.22	55.69	88.47	92.65	80.06	55.96	48.09	72.80	98.45	89.27	100.35	146.34

dr_i (%) when considering TiO_2 as conserved

i	SiO_2	TiO_2	Al_2O_3	FeO	Fe_2O_3	MnO	MgO	CaO	Na_2O	K_2O	P_2O_5	Sc	Li	Rb	Sr	Zr
Alter 1	-8.06	0.00	-9.69	-12.21	-6.45	-56.20	-17.29	-13.84	-21.66	-47.63	-48.67	-12.06	-18.92	-18.03	-16.67	0.00
Alter 2	-17.25	0.00	-20.97	-34.15	-29.84	-64.96	-37.97	-56.92	-47.78	-58.11	-58.69	-4.52	-32.43	-28.28	-27.08	0.00
Alter 3	-26.45	0.00	-32.26	-45.13	-41.53	-73.72	-48.31	-64.10	-60.83	-68.58	-68.70	-12.06	-45.95	-38.52	-37.50	0.00
Alter 4	10.33	0.00	7.25	9.74	16.93	31.39	13.72	14.88	17.51	30.92	51.49	25.63	45.24	22.95	14.58	0.00
Alter 5	19.52	0.00	12.89	31.69	40.32	75.19	45.10	29.24	30.56	57.10	101.56	50.75	21.62	43.44	25.00	0.00
Alter 6	28.72	0.00	18.54	53.64	63.71	118.99	44.74	43.60	56.67	109.47	151.64	75.88	35.14	53.69	35.42	0.00
Alter 7	37.91	0.00	24.18	75.59	87.10	162.78	65.41	57.96	82.79	161.83	201.72	101.01	48.65	63.93	45.83	0.00

dr_i (%) when considering Zr as conserved

i	SiO_2	TiO_2	Al_2O_3	FeO	Fe_2O_3	MnO	MgO	CaO	Na_2O	K_2O	P_2O_5	Sc	Li	Rb	Sr	Zr
Alter 1	-8.06	0.00	-9.69	-12.21	-6.45	-56.20	-17.29	-13.84	-21.66	-47.63	-48.67	-12.06	-18.92	-18.03	-16.67	0.00
Alter 2	-17.26	0.00	-20.98	-34.16	-29.84	-64.96	-37.97	-56.92	-47.78	-58.11	-58.69	-4.53	-32.43	-28.28	-27.09	0.00
Alter 3	-26.45	0.00	-32.27	-45.13	-41.53	-73.72	-48.31	-64.10	-60.83	-68.58	-68.70	-12.06	-45.95	-38.53	-37.50	0.00
Alter 4	10.33	0.00	7.24	9.74	16.93	31.39	13.72	14.87	17.50	30.91	51.48	25.62	45.21	22.95	14.58	0.00
Alter 5	19.52	0.00	12.89	31.69	40.32	75.18	45.10	29.23	30.56	57.09	101.56	50.75	21.62	43.44	25.00	0.00
Alter 6	28.71	0.00	18.53	53.63	63.70	118.98	44.73	43.59	56.67	109.46	151.63	75.87	35.13	53.68	35.41	0.00
Alter 7	37.91	0.00	24.18	75.58	87.09	162.77	65.41	57.95	82.78	161.82	201.71	101.00	48.64	63.93	45.83	0.00

Table 2 continued.

dr_i (%) when considering Al_2O_3 as conserved

i	SiO_2	TiO_2	Al_2O_3	FeO	Fe_2O_3	MnO	MgO	CaO	Na_2O	K_2O	P_2O_5	Sc	Li	Rb	Sr	Zr
Alter 1	1.80	10.72	0.00	-2.79	3.58	-51.51	-8.42	-4.60	-13.26	-42.09	-43.85	-2.63	-10.22	-9.24	-7.73	10.72
Alter 2	4.71	26.54	0.00	-16.68	-11.22	-55.66	-21.51	-45.49	-33.91	-47.06	-48.66	20.82	-14.50	-9.24	-7.73	26.54
Alter 3	8.59	47.63	0.00	-18.99	-13.68	-61.20	-23.69	-47.00	-42.17	-53.67	-55.08	29.83	-20.20	-9.24	-7.73	47.63
Alter 4	2.87	-6.76	0.00	2.33	9.03	22.51	6.04	7.11	9.56	21.91	41.86	17.14	0.80	14.64	6.84	-6.76
Alter 5	5.87	-11.42	0.00	16.65	24.30	55.18	9.89	14.48	15.65	38.98	79.68	33.54	7.73	27.06	10.72	-11.42
Alter 6	8.59	-15.64	0.00	29.61	38.11	84.74	22.10	21.14	32.17	76.48	113.91	48.37	14.00	29.65	14.24	-15.64
Alter 7	11.06	-19.47	0.00	41.40	50.66	111.61	33.20	27.20	47.19	110.57	145.02	61.86	19.70	32.01	17.43	-19.47

dr_i (%) when considering Sr as conserved

i	SiO_2	TiO_2	Al_2O_3	FeO	Fe_2O_3	MnO	MgO	CaO	Na_2O	K_2O	P_2O_5	Sc	Li	Rb	Sr	Zr
Alter 1	10.33	20.00	8.38	5.35	12.26	-47.44	-0.75	3.39	-6.00	-37.24	-39.14	5.53	-2.70	-1.64	0.00	20.00
Alter 2	13.48	37.14	8.38	-9.70	-3.78	-51.95	-14.93	-40.92	-28.38	-42.62	-44.36	30.94	-7.34	-1.64	0.00	37.14
Alter 3	17.68	60.00	8.38	-12.21	-6.45	-57.95	-17.29	-42.56	-37.33	-49.79	-51.32	40.70	-13.51	-1.64	0.00	60.00
Alter 4	-3.71	-12.73	-6.40	-4.22	2.05	14.67	-0.75	0.26	2.55	14.10	32.78	9.64	-5.65	7.30	0.00	-12.73
Alter 5	-4.38	-20.00	-9.69	5.35	12.26	40.15	-0.75	3.39	4.45	25.51	62.28	20.60	-2.70	14.75	0.00	-20.00
Alter 6	-4.95	-26.15	-12.46	13.46	20.89	61.71	6.88	6.04	15.70	54.48	87.25	29.88	-0.21	13.49	0.00	-26.15
Alter 7	-5.43	-31.43	-14.85	20.40	28.29	80.19	13.43	8.31	25.34	79.31	108.65	37.83	1.93	12.41	0.00	-31.43

dr_i (%) when considering P_2O_5 as conserved

i	SiO_2	TiO_2	Al_2O_3	FeO	Fe_2O_3	MnO	MgO	CaO	Na_2O	K_2O	P_2O_5	Sc	Li	Rb	Sr	Zr
Alter 1	81.30	97.19	78.09	73.12	84.47	-13.64	63.09	69.90	54.47	3.13	0.00	73.41	59.88	61.63	64.32	97.19
Alter 2	103.96	146.49	94.79	62.30	72.94	-13.64	52.90	6.18	28.73	3.13	0.00	135.34	66.54	76.78	79.73	146.49
Alter 3	141.73	228.65	122.61	80.33	92.15	-13.64	69.89	17.98	28.73	3.13	0.00	189.01	77.65	102.04	105.41	228.65
Alter 4	-27.48	-34.27	-29.51	-27.87	-23.14	-13.64	-25.25	-24.49	-22.76	-14.06	0.00	-17.42	-28.94	-19.18	-24.68	-34.27
Alter 5	-41.08	-50.70	-44.35	-35.08	-30.83	-13.64	-38.84	-36.29	-35.64	-22.66	0.00	-25.68	-40.04	-29.29	-38.38	-50.70
Alter 6	-49.24	-60.56	-53.25	-39.41	-35.44	-13.64	-42.92	-43.37	-38.21	-17.50	0.00	-30.64	-46.71	-39.39	-46.59	-60.56
Alter 7	-54.68	-67.14	-59.19	-42.29	-38.51	-13.64	-45.64	-48.09	-39.93	-14.06	0.00	-33.94	-51.15	-46.12	-52.07	-67.14

The element masses for each of the eight numerically generated samples are presented in figure 1 (TiO_2 and Zr have the same masses for all samples because of their conserved assumption; see above). When these element masses are transformed into concentrations (Fig. 2), the element concentrations in the daughter samples underwent either enrichment or dilution when compared to those of the parent rock, no matter if the element was actually conserved or not (cf. Fig. 1). This means, not only did the system size of the rocks change, but also did all the element concentrations (Fig. 2), particularly TiO_2 and Zr. It is worth noting that SiO_2, Al_2O_3, TiO_2 and Zr decreased in samples that have added mass, while the rest of the other elements displayed an overall gradual enrichment (Fig. 2).

Estimated Isomass results are presented in figure 3 (data provided in Table 2). Table 2 includes Isomass results for TiO_2, Zr and Al_2O_3 as possible conserved elements, considering daughter system sizes (S_{dk}) and relative material transfer (dr_i). Note that results for TiO_2 and Zr are identical, with their dr_i values being 0, which makes sense because these two elements are actually conserved. In fact, TiO_2 suffers no material transfer when Zr is assumed to be conserved and vice versa. Furthermore, the relative material transfer percentage for any other element is exactly the same whether calculated with Zr of TiO_2. In contrast, when a non-conserved element (*e.g.*, Al_2O_3, Sr, P_2O_5) is assumed to be conserved, no other element is predicted to be conserved (Fig. 3), which means that all of the calculated relative material

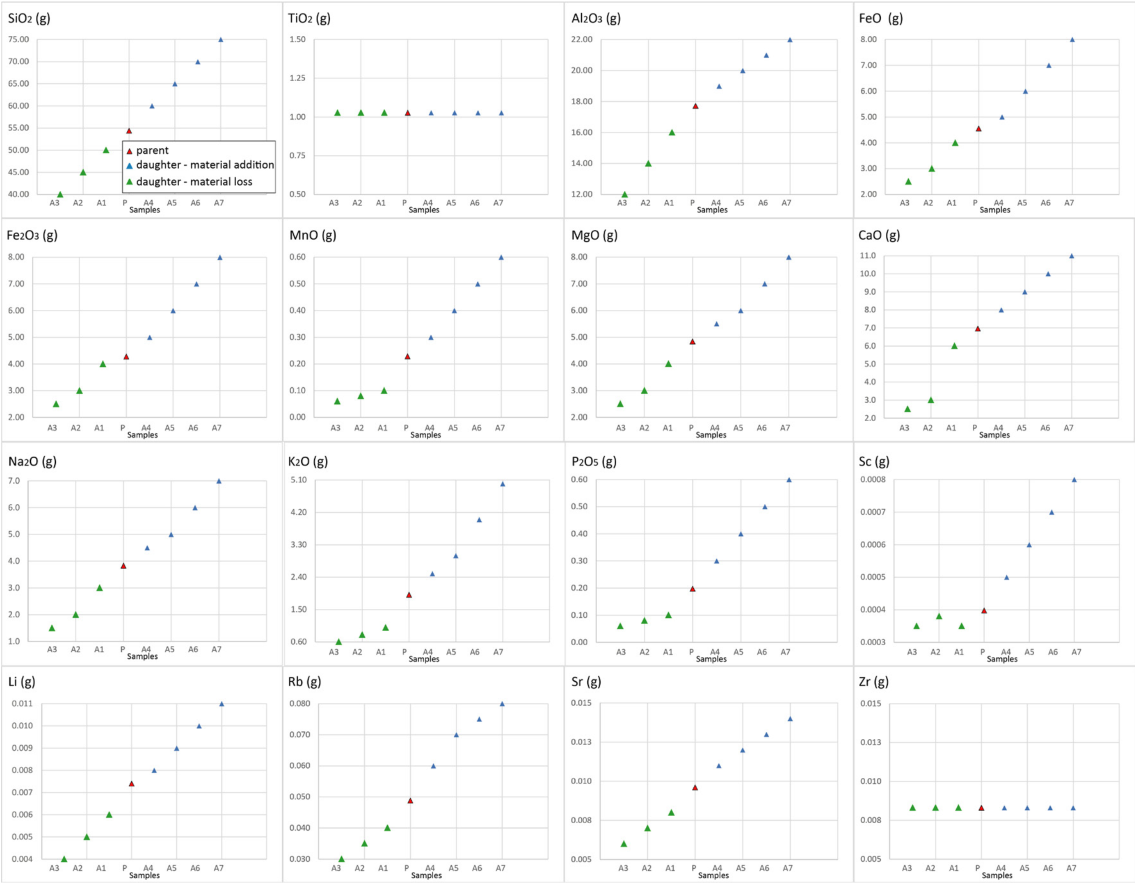

FIG. 1. Masses of major oxide and trace elements for the numerically generated dataset. Red triangle: parent sample. Green triangles: daughter samples that lost mass relative to the parent sample. Blue triangles: daughter samples that gained mass relative to the parent sample. See table 1 for calculation details.

FIG. 2. Concentrations of major oxide and trace elements for the numerically generated dataset. See table 1 for calculation details. Symbols as in figure 1.

transfers dr_i are wrong (*e.g.*, P_2O_5 material transfers predicted in figure 3 are contrary to the actual material transfer tendencies presented in figure 1). These calculations do not validate conservation because the prior conserved assumption is not confirmed by a second conserved element. In consequence, element conservation cannot be validated when only one conserved element exists. At least two such elements are therefore required.

Following the above reasoning, when a pair of elements k_1 and k_2 are plotted on a S_{di}/S_{dk_1} versus S_{di}/S_{dk_2} diagram, the daughter system size ratios for the conserved element will plot at unity for all samples, and when both elements are conserved, all plotted data will fall in a line with a unity slope. In addition, if the element in the ordinate denominator is a conserved element, samples with loss of material will plot below the unity line trend, whereas those with material gain will plot above the unity line trend.

Figure 4 presents the daughter system size ratios for the same sixteen elements presented in figure 3 compared with the daughter system sizes for S_{di}/S_{dTiO_2} (vertical axes) and $S_{di}/S_{d\mathrm{Zr}}$, $S_{di}/S_{dAl_2O_3}$, $S_{di}/S_{d\mathrm{Sr}}$ and $S_{di}/S_{dP_2O_5}$ (horizontal axes) shown in table 2. Results indicate that only the conservated element pair (TiO_2-Zr; upper left panel) estimates the same rock sizes for every sample. Although other element pairs display relatively high correlation coefficients (*e.g.*, Al_2O_3), the data define trends with slopes that depart from unity and/or have intercepts far from zero. The plots for $S_{di}/S_{d\mathrm{TiO_2}}$ vs. $S_{di}/S_{dAl_2O_3}$, $S_{di}/S_{d\mathrm{TiO_2}}$ versus $S_{di}/S_{d\mathrm{Sr}}$, and $S_{di}/S_{d\mathrm{TiO_2}}$ vs. $S_{di}/S_{dP_2O_5}$ show that the estimated daughter system size ratios are higher than 1 in samples A1-A3 and lower than 1 in samples A4-A7.

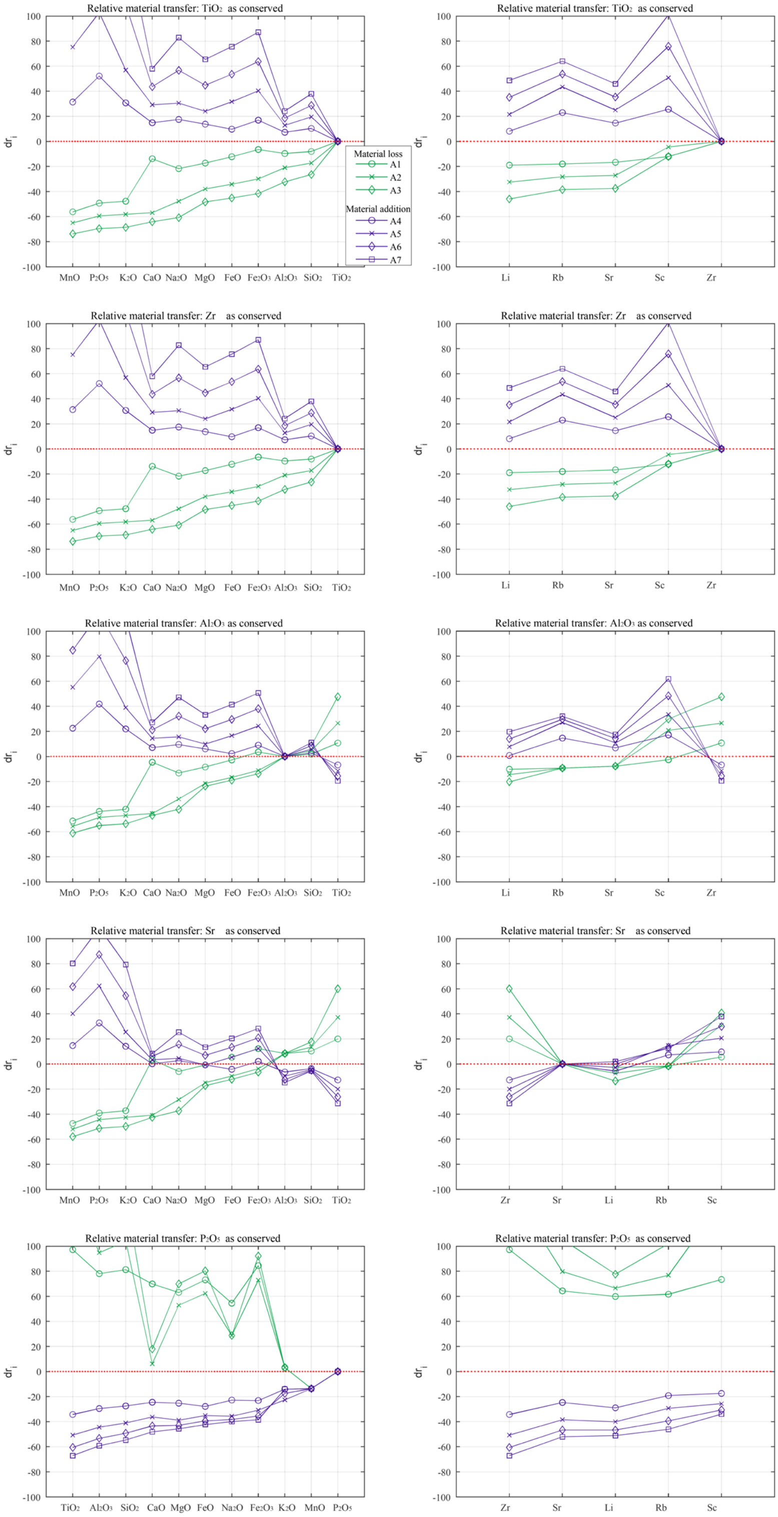

FIG. 3. Relative material transfer percentages for the numerically generated dataset considering TiO_2, Zr, Al_2O_3, Sr, and P_2O_5 as conserved elements. Left panels show major elements. Right panels indicate trace elements. In green, samples that lost mass. In blue, samples that gained mass. Red line represents parent composition. See table 2 for calculation details.

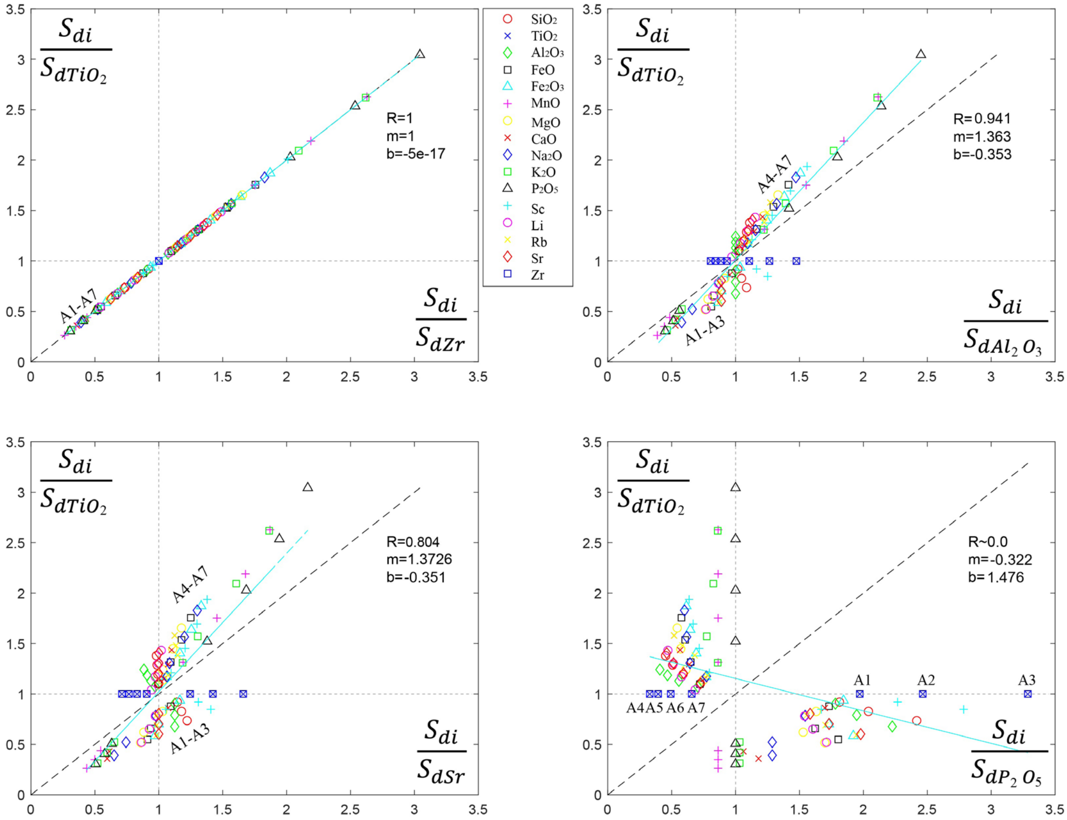

FIG. 4. Daughter system size ratios for TiO_2 versus Zr, TiO_2 versus Al_2O_3, TiO_2 versus Sr, and TiO_2 versus P_2O_5 for the numerically generated dataset. R: correlation coefficient; m: slope of the trend line; b: intercept with the y-axis. Cyan line: trend line. Dashed black line: slope of unity, intercept at the origin. See table 2 for calculation details.

When, by these means, it is not possible to identify a pair of conserved elements, it is suggested to use as nearly conserved elements those elements displaying the closest results to the conserved element pair behaviour. This is: the closest distribution of data to the unity slope in a daughter system size ratios diagram. In case a pair of non-conserved elements show identical concentration changes, they will depart from the unity slope line yet will still display a highly correlated distribution. This is because elements that show coherent mobility (proportional concentration changes) do not necessarily reflect proportional mass changes.

The example from above illustrates that concentrations alone do not accurately describe the behaviour of element material transfers when affected by geochemically open geological processes. Such material transfers can be calculated by using the Isomass method when elements actually conserved can be identified. The detailed Isomass calculations are present in Supplementary material 2.

3.2. Real cases

The real-case datasets investigate material transfer associated with soil development (Jiang *et al.*, 2018), magmatic fractionation (Shore, 1996), and hydrothermal metasomatism (Mori *et al.*, 2003). The background information and conserved elements validated by the Isomass method are summarized in table 3. Although numerous geological examples of material transfer are available in the literature (Alderton *et al.*, 1980; Smith *et al.*, 1982; Aguirre, 1988; Ague, 1991; Magloughin, 1992; Goddard, 1993; Condie *et al.*, 1995; Christidis, 1998; Bach, 2001; Oliver *et al.*, 2004; Malviya *et al.*, 2006;

TABLE 3. BACKGROUND INFORMATION AND SUMMARIZED ISOMASS RESULTS FOR THE REAL-CASE STUDIES.

Geological Process	Author	Age-Locality	Materials	Minerals	Process	Conserved elements
Soil development	Jiang *et al.* (2018)	Mio-Pliocene, Hainan Island (China)	Soil, saprolite, semiweathered basalt, tholeiitic basalt	Kaolinite, iron oxyhydroxides, gibbsite, bohemite	Desilication, ferralitization	TiO_2-Hf
Magmatic fractionation	Shore (1996)	~2710 Ma, Ontario (Canada)	Komatiite lava (flow C)	Olivine, spinel, augite, pigeonite, serpentine, glass	Cooling and crystallization of a lava flow	Al_2O_3-V
Hydrothermal metasomatism	Mori *et al.* (2003)	Late Cretaceous, Nishisonogi (Japan)	Epidote blue schists	Winchite, epidote, chlorite, calcite, albite, quartz, amphibole, illite, dolomite	Retrograde dolomite-calcite vein in basic schist	Cr-Sc-V

Liu *et al*., 2016), the specific studies mentioned above were chosen due to the large number of elements analysed, good knowledge about the mobility that these elements underwent, and the presence of a conserved element.

In the first example, data from a >15 m-thick soil/saprolite profile from a weathered tholeiitic basalt was tested with the Isomass method. This basalt was affected by silica loss and iron oxidation during weathering in an extreme tropical climate on the island of Hainan (South China). The mineral assemblage is dominated by Fe-oxides/hydroxides and gibbsite (or boehmite), and the authors (Jiang *et al*., 2018) tested the hypothesis that Nb was the most stable immobile element.

The second example involves the cooling and crystallization history of komatiitic lava flows in Munro, Ontario, Canada. These flows were affected by seawater convection that caused both cooling and fracturing, resulting in the serpentinization of the rocks. Magnesium-rich olivine crystallization dominated the fractionation process, and the author (Shore, 1996) hypothesized that Th was conserved.

The third and last example involves rocks that were intruded by carbonate veins. Analysed by Mori *et al*. (2003) using the Isocon method, they concluded that Cr, Sc, V, Al, and Ti were conserved or nearly conserved elements. They studied the material transfer reaction paths in alteration zones around dolomite-calcite veins in basic schists affected by epidote-blueschist metamorphism at Nishisonogi, southwest Japan.

After running the Isomass code (Supplementary material 1) for these real-case examples, TiO_2 and Hf were identified as conserved for the saprolite profile, Al_2O_3 and V were for the komatiite lavas, and Cr and V for the basic schists. Figure 5 illustrates the relative material transfer percentages for TiO_2, Al_2O_3, and Cr, whereas the daughter system size ratios for the conserved element pairs are shown in figure 6.

The patterns displayed in figure 5 are different in each case due to differences in parent rock compositions and the processes affecting daughter samples. All element pairs identified as conserved by the Isomass method produce the expected conserved element behaviours on both plots (Figs. 5 and 6). However, some of the elements originally thought to be conserved by the former authors were not confirmed as conserved in our case study application.

The data displayed in figure 5A, B illustrate that material transfer processes are mainly controlled by the removal of mass via leaching of almost all major elements, with the exception of Al_2O_3 and Fe_2O_3. Material transfer of trace elements is more diverse, with alkali and alkaline earth elements strongly lost (dr_i below -60%), transition metals moderately lost (dr_i between -60 and -20%) or added (dr_i between 20% and 60%), and high field strength elements weakly lost or added (dr_i between -20% and 20%). Overall, material transfer in this saprolite example displays expected patterns consistent with tropical weathering, with almost complete loss of Na_2O, CaO, K_2O, and MgO, minor loss of SiO_2, and residual enrichment of Fe_2O_3 and Al_2O_3.

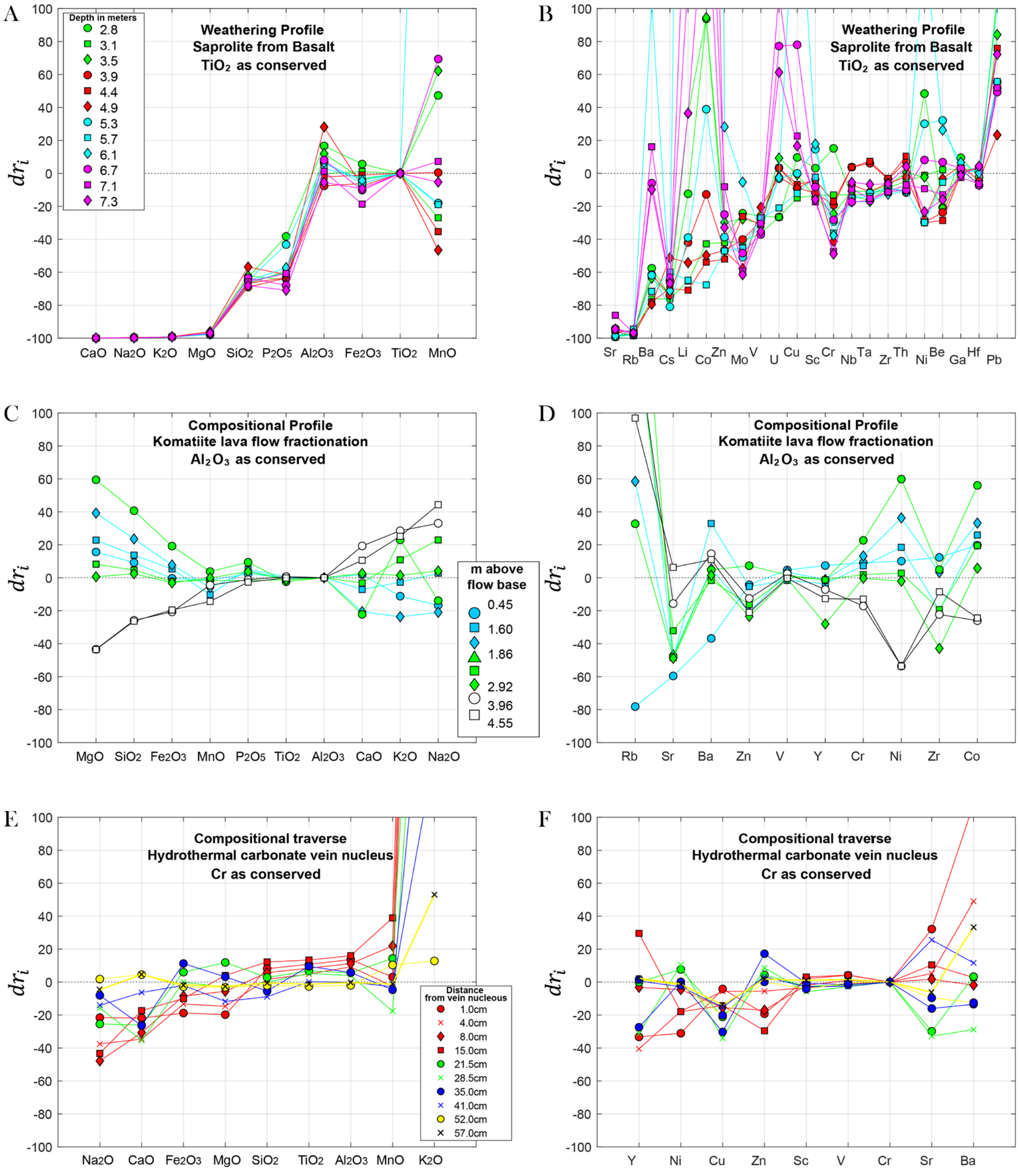

FIG. 5. Relative material transfer percentages for the real-case datasets, considering TiO_2, Al_2O_3, and Cr as conserved elements (see text for explanation). Left panels show major elements. Right panels indicate trace elements. **A-B**. Soil depth (in meters) from a saprolite weathering profile (parent material: basalt) (Jiang *et al*., 2018). **C-D**. Different levels (reported as meters above base) in komatiitic lava flow (Shore, 1996). **E-F**. Traverse (in centimetres) along a hydrothermal carbonate vein nucleus (Mori *et al*., 2003). See Supplementary material 2 for calculation details.

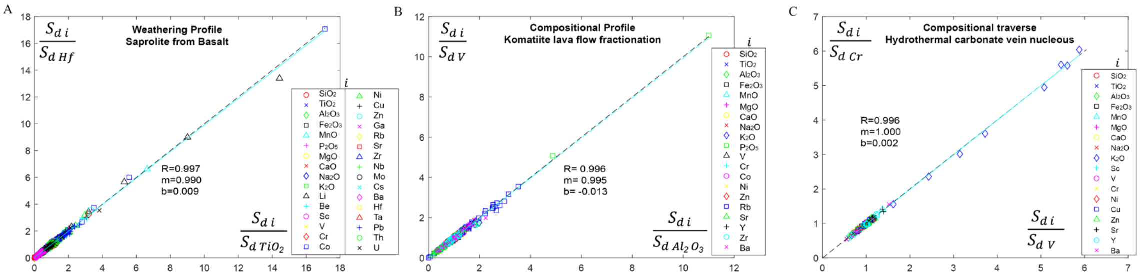

FIG. 6. Daughter system size ratios for Hf versus TiO_2, V versus Al_2O_3, and Cr versus V for the real-case datasets. **A**. Saprolite weathering profile (Jiang *et al*., 2018). **B**. Komatiitic lava flow (Shore, 1996). **C**. Hydrothermal carbonate vein (Mori *et al*., 2003). R: correlation coefficient; m: slope of the trend line; b: intercept with the y-axis. Cyan line: trend line. Dashed black line: slope of unity, intercept at the origin. See Supplementary material 2 for calculation details.

The patterns in the komatiitic lava flow are consistent with the sampling levels within the flow (Fig. 5C, D). Larger material transfer occurs in MgO and SiO_2 (consistent with olivine fractionation) as well as in K_2O and Na_2O (consistent with post-emplacement alteration). The same tendencies are reflected in trace elements by Ni-Cr-Co and Rb-Ba-Sr, so magmatic differentiation processes are interpreted to generate these patterns.

Lastly, the hydrothermal alteration around carbonate veins does not indicate substantial material transfer, as dr_i are generally below ±40% (Fig. 5E, F). Nevertheless, some concentration patterns can be observed adjacent to the vein, with K_2O and Ba added proximally, and Cu lost distally. Na_2O and CaO are systematically lost almost everywhere, and SiO_2, TiO_2 and Al_2O_3 are almost conserved, exhibiting only minor addition to the adjacent rocks.

The examples illustrated above suggest that any changes in the size of the systems that underwent geochemically open processes can be identified by using the Isomass method. By knowing the size of systems, the actual material transfer effects on rock chemistry caused by these processes can be elucidated.

5. Discussion and conclusions

The Isomass method allows the validation of conserved elements, and thus provides measures of material transfer which can be compared to Pearce Element Ratio (PER) analyses. In fact, they match almost exactly, as the Pearce Element Ratio diagrams are an effective means of portraying element variations within igneous rock suites and interpreting the causes of chemical diversity assuming a conserved element (Russell *et al*., 1990). The Isomass method can prevent errant interpretations sourced from methods that identify conserved elements on a petrological basis or from chemical concentration trends, not considering therefore the possibility of using a non-conserved element in material transfer calculations.

The Isomass method firstly involves the estimation of the daughter system size (S_{di}), from which an estimate of the relative material transfer (dr_i) can be made. The sum of squares of these relative material transfers for all the elements analysed provides a quantitative measure of the conserved character of every element. Figure 7 illustrates how a conserved (or nearly conserved) group of elements minimizes the relative material transfer sum of squares (*e.g.*, Sc-V-Cr in the hydrothermal alteration case). This latter procedure identifies the elements most involved in material transfer.

After deciding which elements are conserved (dX_k=0), the behaviour of other non-conserved elements can be estimated by means of the daughter system size ratios. This allows a graphical comparison of the S_{di}/S_{dk} between a pair of theoretically conserved elements, and is an extension of and an alternative to the Isocon method applied to all available samples, as it explicitly compares the S_{di} estimate of any element to the S_{dk} estimate of the hypothetically conserved element.

In case the rocks densities are known, it is possible to calculate the real volume changes that occurred and compare these with the mineral compositions and/or the chemical reactions thought to be responsible of the observed geological processes. This can provide an additional way to validate the Isocon method results.

The Isomass method can be a useful approach to the task of validating conserved elements in a rock suite. It provides a strategy to visualize the changes

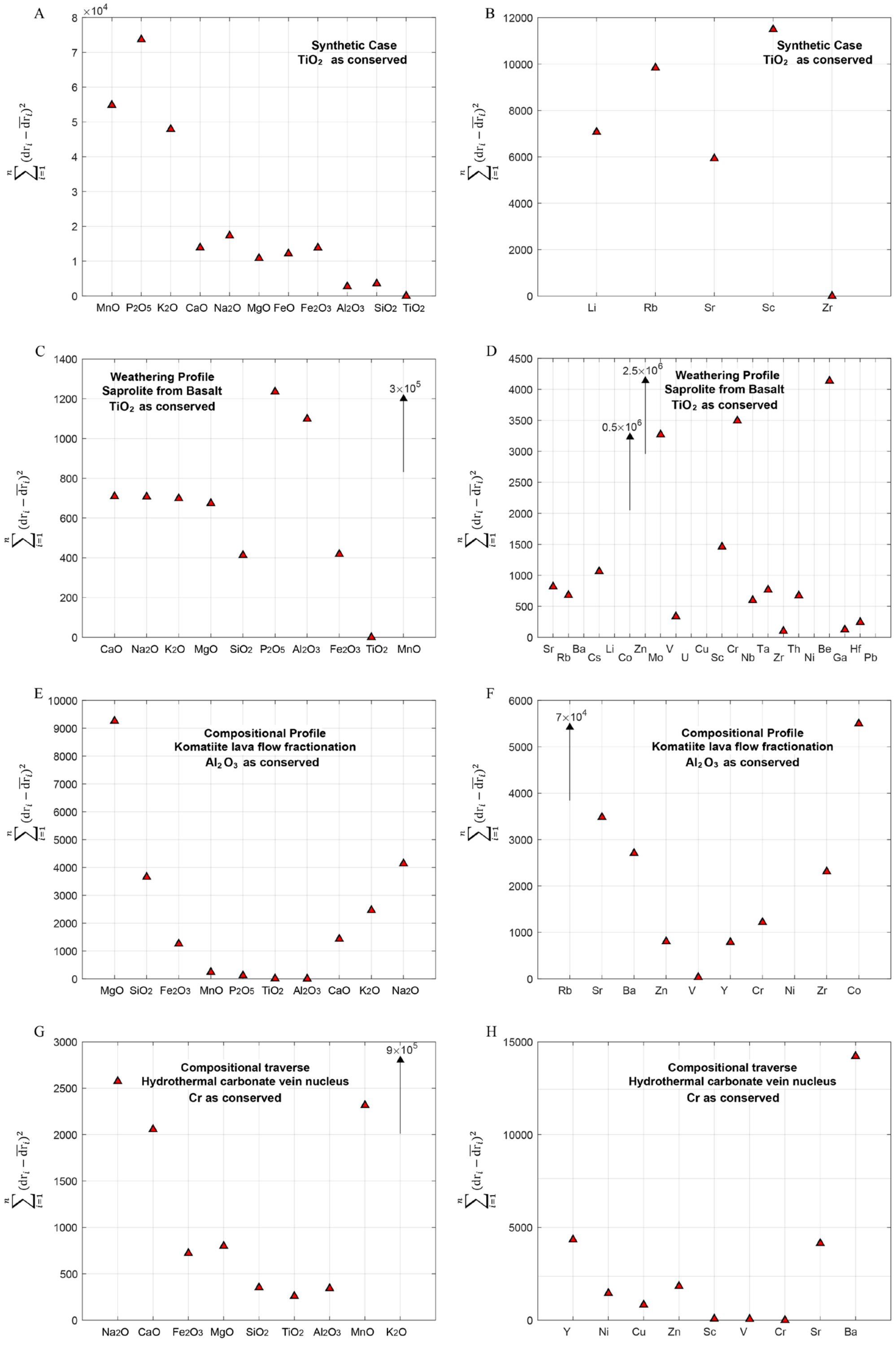

FIG. 7. Sum of squares of estimates for the numerically generated case (**A**, **B**), soil profile (**C**, **D**), komatiitic lava (**E**, **F**), and hydrothermal (**G**, **H**) examples. A conserved (or nearly conserved) group of elements will plot near the zero value.

that a given element undergoes with respect to an element assumed to be conserved. In the process, the Isomass method makes it possible to calculate all element mass changes in rocks affected by geochemically open processes.

By modifying the mass balance equation proposed by Grant (1986), we were able to obtain quantitative estimates of individual mass changes for every element in a system affected by a material transfer process. These system changes affect the volume and density of the rocks and provide hints on the actual process (or processes) involved in material transfer. The interpretation based on whole-rock analysis is therefore limited by the analytical availability of elements, the analytical technique used (the total analytical error), the homogeneity and representativity of the rock samples, and the identification of which samples represent the parent rock best.

In the Isomass method, the larger the number of elements available and analysed, the greater the certainty of the results. Likewise, when more parent samples are available, there is more accuracy in the identification of the conserved elements. In addition, despite the impact of system closure on rock compositions, the Isomass method circumvents such potential problems by providing a clear understanding of the material transfer for each element of interest.

Any changes in the whole-rock chemical composition during a geochemically open process produce concentration changes caused by absolute material transfer that can be diverse and complicated. The Isomass method thus provides a pathway to whole-rock chemical data interpretation which can be utilized when a conserved element is available. In conclusion, the Isomass method represents a powerful quantitative tool to understand the mass transfer processes reflected by whole-rock compositional variations. This technique can be applied to any material transfer process, no matter if the cause is magmatic, metamorphic or hydrothermal.

Acknowledgments

We acknowledge the assistance provided to the authors by the technical and administrative team of the Department of Geology, University of Chile. Funding for this work was supplied by the National Agency for Research and Development, Chile [ANID grant 21080725 / Formerly Science and Technology National Commission -CONICYT]. D. Sellés and an anonymous reviewer help revising this manuscript. Special acknowledgments to L. Aguirre Le-Bert and F. Hervé Allamand for their contribution to metamorphic geology understanding. Additional information is available in Supplementary material 1 and 2.

References

Ague, J.J. 1991. Evidence for major mass transfer and volume strain during regional metamorphism of pelites. Geology 19 (8): 855-858. https://doi.org/10.1130/0091-7613(1991)019%3C0855:EFMMTA%3E2.3.CO;2

Aguirre, L. 1988. Chemical mobility during low grade metamorphism of a Jurassic lava flow: Río Grande Formation, Peru. Journal of South American Earth Sciences 1 (4): 343-361. https://doi.org/10.1016/0895-9811(88)90022-3

Alderton, D.H.M.; Pearce, J.A.; Potts, P.J. 1980. Rare earth element mobility during granite alteration: evidence from southwest England. Earth and Planetary Science Letters 49 (1): 149-165. https://doi.org/10.1016/0012-821X(80)90157-0

Baumgartner, L.P.; Olsen, S.N. 1995. A Least-Squares Approach to Mass Transport Calculation Using the Isocon Method. Economic Geology 90: 1261-1270. https://doi.org/10.2113/gsecongeo.90.5.1261

Bach, W.; Alt, J.C.; Niu, Y.; Humphris, S.E.; Erzinger, J.; Dick, H.J.B. 2001. The geochemical consequences of late-stage low-grade alteration of lower ocean crust at the SW Indian Ridge: Results from ODP Hole 735B (Leg 176). Geochimica et Cosmochimica Acta 65 (19): 3267-3287. https://doi.org/10.1016/S0016-7037(01)00677-9

Brinkley, S.R. 1946. Note on the conditions of equilibrium for systems of many constituents. Journal of Chemical Physics 14: 563-564. https://doi.org/10.1063/1.1724195

Brinkley, S.R. 1947. Calculation of the equilibrium composition of systems of many constituents. Journal of Chemical Physics 15: 107-110. https://doi.org/10.1063/1.1746420

Coelho, J. 2006. GEOISO-A WindowsTM program to calculate and plot mass balances and volume changes occurring in a wide variety of geologic processes. Computers & Geosciences 32 (9): 1523-1528. https://doi.org/10.1016/j.cageo.2006.01.008

Condie, K.C.; Dengate, J.; Cullers, R.L. 1995. Behavior of rare earth elements in a paleoweathering profile on granodiorite in the Front Range, Colorado, USA. Geochimica et Cosmochimica Acta 59 (2): 279-294. https://doi.org/10.1016/0016-7037(94)00280-Y

Christidis, G.E. 1998. Comparative study of the mobility of major and trace elements during alteration of an andesite and a rhyolite to bentonite, in the islands of

Milos and Kimolos, Aegean, Greece. Clays and Clay Minerals 46 (4): 379-399. https://doi.org/10.1346/CCMN.1998.0460403

Giggenbach, W.F. 1984. Mass transfer in hydrothermal alteration systems-A conceptual approach. Geochimica et Cosmochimica Acta 48 (12): 2693-2711. https://doi.org/10.1016/0016-7037(84)90317-X

Ghiorso, M.S. 1985. Chemical mass transfer in magmatic processes I. Thermodynamic relations and numerical algorithms. Contributions to Mineralogy and Petrology 90: 107-120. https://doi.org/10.1007/BF00378254

Goddard, J.V. 1993. Internal deformation, evolution and fluid flow in basement involved thrust faults, Norwest Wyoming. M.Sc. Thesis (Unpublished), Utah State University: 145 p. Logan. https://doi.org/10.26076/2994-e057

Grant, J.A. 1986. The Isocon diagram-A simple solution to Gresens' equation for metasomatic alteration. Economic Geology 81: 1976-1982. https://doi.org/10.2113/gsecongeo.81.8.1976

Grant, J.A. 2005. Isocon analysis: A brief review of the method and applications. Physics and Chemistry of the Earth 30 (17-18): 997-1004. https://doi.org/10.1016/j.pce.2004.11.003

Gresens, R.L. 1967. Composition-volume relationships of metasomatism. Chemical Geology 2: 47-55. https://doi.org/10.1016/0009-2541(67)90004-6

Guo, S.; Ye, K.; Chen, Y.; Liu, J.B. 2009. A normalization solution to mass transfer illustration of multiple progressively altered samples using the Isocon diagram. Economic Geology 104 (6): 881-886. https://doi.org/10.2113/gsecongeo.104.6.881

Hilchie, L.; Russell, J.K.; Stanley, C.R. 2018. Unification of Isocon and Pearce Element Ratio techniques in the quantification of material transfer. Economic Geology 113 (7): 1603-1608. https://doi.org/10.5382/econgeo.2018.4605

Jiang, K.; Qi, H.; Hu, R. 2018. Element mobilization and redistribution under extreme tropical weathering of basalts from the Hainan Island, South China. Journal of Asian Earth Sciences 158: 80-102. https://doi.org/10.1016/j.jseaes.2018.02.008

Karpov, I.; Chudnenko, K.; Kulik, D. 1997. Modelling chemical mass transfer in geochemical processes: thermodynamic relations, conditions of equilibrium, and numerical algorithms. American Journal of Sciences 297 (8): 767-806. https://doi.org/10.2475/ajs.297.8.767

Liu, W.; Liu, C.; Brantley, S.L.; Xu, Z.; Zhao, T.; Liu, T.; Yu, Ch.; Xue, D.; Zhao, Z.; Cui, L.; Zhang, Z.; Fan, B.; Gu, X. 2016. Deep weathering along a granite ridgeline in a subtropical climate. Chemical Geology 427: 17-34. https://doi.org/10.1016/j.chemgeo.2016.02.014

MacLean, W.H. 1990. Mass change calculations in altered rock series. Mineralium Deposita 25 (1): 44-49. https://doi.org/10.1007/BF03326382

MacLean, W.H.; Barrett, T.J. 1993. Lithogeochemical techniques using immobile elements. Journal of Geochemical Exploration 48 (2): 109-133. https://doi.org/10.1016/0375-6742(93)90002-4

Maclean, W.H.; Kranidiotis, P. 1987. Immobile elements as monitors of mass transfer in hydrothermal alteration: Phelps Dodge massive sulfide deposit, Matagami, Quebec (Canada). Economic Geology 82 (4): 951-962. https://doi.org/10.2113/gsecongeo.82.4.951

Magloughlin, J.F. 1992. Microstructural and chemical changes associated with cataclasis and frictional melting at shallow crustal levels: the cataclasite-pseudotachylyte connection. Tectonophysics 204 (3-4): 243-260. https://doi.org/10.1016/0040-1951(92)90310-3

Malviya, V.P.; Arima, M.; Pati, J.K.; Kaneko, Y. 2006. Petrology and Geochemistry of metamorphosed basaltic pillow lava and basaltic komatiite in the Mauranipur area: subduction related volcanism in the Archean Bundelkhand craton, Central India. Journal of Mineralogical and Petrological Sciences 101 (4): 199-217. https://doi.org/10.2465/jmps.101.199

Mori, Y.; Nishiyama, T.; Yanagi, T. 2003. Mass transfer and reaction paths in alteration zones around carbonate veins in the Nishisonogi Metamorphic Rocks, southwest Japan. American Mineralogist 88 (4): 611-623. https://doi.org/10.2138/am-2003-0415

Mukherjee, P.K.; Gupta, P.K. 2007. Arbitrary scaling in ISOCON method of geochemical mass balance: An evaluation of the graphical approach. Geochemical Journal 42 (3): 247-253. https://doi.org/10.2343/geochemj.42.247

Oliver, N.H.S; Cleverley, J.S.; Mark, G.; Pollard, P.; Fu, B.; Marchall, L.J.; Rubenach, M.J.; Williams, P.; Baker, T. 2004. Modeling the Role of Sodic Alteration in the Genesis of Iron Oxide-Copper-Gold Deposits, Eastern Mount Isa Block, Australia. Economic Geology 99 (6): 1145-1176. https://doi.org/10.2113/gsecongeo.99.6.1145

Pearce T.H. 1968. A Contribution to the Theory of Variation Diagram. Contributions to Mineralogy and Petrology 19: 142-157. https://doi.org/10.1007/BF00635485

Russell, J.K.; Nicholls, J. 1988. Analysis of petrologic hypotheses with Pearce element ratios. Contributions to Mineralogy and Petrology 99 (1): 25-35. https://doi.org/10.1007/BF00399362

Russell, J.K.; Stanley, C.R. 1990. A theoretical basis for the development and use of chemical variation diagrams. Geochimica et Cosmochimica Acta 54 (9): 2419-2431. https://doi.org/10.1016/0016-7037(90)90229-E

Russell, J.K.; Nicholls, J.; Stanley, C.R.; Pearce, T.H. 1990. Pearce element ratios: A paradigm for testing hypotheses. Eos 71 (5): 234-247. https://doi.org/10.1029/EO071i005p00234

Shore, M. 1996. Cooling and crystallization of komatiite flows. Ph.D. Thesis (Unpublished), University of Ottawa: 211 p. Ottawa. http://hdl.handle.net/10393/10267

Smith, R.E.; Perdrix, J.L.; Parks, T.C. 1982. Burial Metamorphism in the Hamersley Basin, Western Australia. Journal of Petrology 23 (1): 75-102. https://doi.org/10.1093/petrology/23.1.75

Stanley, C.R. 1993. Effects of non-conserved denominators on Pearce Element Ratio diagrams. Mathematical Geology 25: 1049-1070. https://doi.org/10.1007/BF00911549

Stanley, C.R.; Russell, J.K. 1989. PEARCE.PLOT: Interactive graphics-supported software for testing petrologic hypotheses with Pearce element-ratio diagrams. American Mineralogist 74: 273-276.

Vistelius, A.B.; Sarmanov, O.V. 1961. On the correlation between percentage values: major component correlation in ferromagnesium micas. The Journal of Geology 69 (2): 145-153. https://doi.org/10.1086/626725

Manuscript received: May 29, 2023; revised/accepted: November 11, 2024; available online: November 11, 2024.